

An Additional Explanation of the Incisure Origin in the Aortic Pressure Waveform

Ivan KORADE, Zdravko VIRAG, Severino KRIZMANIĆ

**University of Zagreb, Faculty of Mechanical Engineering and Naval
Architecture, Ivana Lučića 5, 10000 Zagreb*

E-mails: [ivan.korade](mailto:ivan.korade@fsb.hr), [zdravko.virag](mailto:zdravko.virag@fsb.hr), [severino.krizmanic](mailto:severino.krizmanic@fsb.hr)@fsb.hr

***Abstract.** The arterial pressure waveform consists of systolic and of diastolic phases. Systolic phase includes blood ejection from the left ventricle into the aorta, which lasts from the aortic valve opening to the valve closing, when the diastolic phase starts. During diastolic phase the aorta is emptying due to blood flow from the aorta to the peripheral vascular beds. These two phases are separated by an incisure in the pressure profile, which includes a sudden pressure drop at the end of systolic phase and a sudden pressure growth at the beginning of diastolic phase. Today's common believe is that the cause of the incisure is a water hammer caused by the aortic valve closing. Further to this interpretation, we hypothesized in this paper that the wall viscosity also contributes to the incisure appearance. Based on the one-dimensional numerical model simulation of blood flow in the arterial tree, we demonstrated that the incisure is deepening by the wall viscosity increase.*

1 Introduction

We investigate an incisure in the aortic pressure profile. Incisure is a result of two phenomena: a sudden pressure drop at the end of systole and a sudden pressure increase at the beginning of diastole. A water hammer phenomena [1, 2, 3], as an incisure origin, is widely accepted. By that, due to the aortic valve closing, there is a reverse blood flow from the aortic root to the left ventricle. This reverse blood flow stops suddenly when the aortic valve closes, causing a sudden pressure growth Δp , defined by the Allievi equation $\Delta p = \rho c \Delta v$ (ρ is the blood density, c is the wave speed and Δv is the change of the reverse blood velocity during the leaflets closing). Based on some theoretical considerations, here we hypothesize that the arterial wall viscosity also contributes to the appearance of the incisure. This additional argumentation could be useful in clinical practice, since the depth of the incisure contains information about the arterial wall viscosity. Although the pressure measurement in the aortic root requires an invasive procedure, which is unacceptable in healthy subjects due to the health risks it brings, it is still possible to observe the incisure non-invasively in the carotid artery by using applanation tonometry.

In the following sections we will provide the mathematical model of one-dimensional (1D) blood flow in the visco-elastic arterial tree, and define the numerical method of characteristics (MOC) for its solving. After that we will explain the hypothesis through a simplified theoretical analysis and finally perform numerical experiments by using the 1D model, which confirms our hypothesis.

2 The Hypothesis

Here we explain the idea for the hypothesis. For this purpose, a simplified lumped parameter (Windkessel) model of blood flow in the aortic root is used. In this model arterial tree is modelled by one chamber in which the pressure distribution is uniform as well as the inlet and outlet flow distributions. Figure 1 shows schematically the aortic root region (also known as the Valsalva sinus) with the definition of inlet flow rate (the aortic valve flow Q_{in}) and outlet flow Q toward the periphery. The continuity equation for the aortic root is:

$$\frac{dV_{ar}}{dt} = Q_{in} - Q, \quad (1)$$

where V_{ar} is the volume of Valsalva sinus, which can be approximated by a cylinder of volume $V_{ar} = A_{ar}L$, where A_{ar} is the characteristic cross-sectional area and L is the equivalent length.

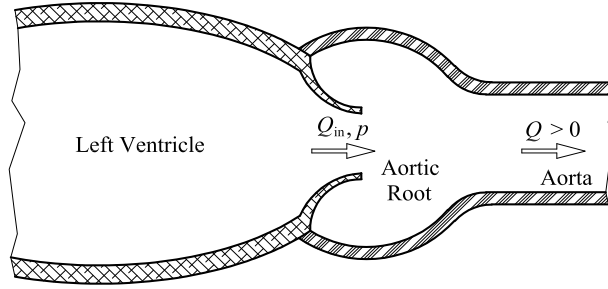


Figure 1: Schematic view of the Valsalva sinus and definition of inlet and outlet flow rates

The aortic wall shows the viscoelastic property, and here it is described by the Voigt model which can be expressed in terms A_{ar} :

$$p = p_e + \eta \frac{dA_{ar}}{dt} = p_e + \frac{\eta}{L} \frac{dV_{ar}}{dt} = p_e + \frac{\eta}{L} (Q_{in} - Q), \quad (2)$$

where p_e is the elastic part of the total pressure, and η is the viscous resistance of the aortic wall. The elastic part of pressure can be defined as:

$$p_e = p_0 + \frac{1}{C} (A_{ar} - A_0) = p_0 + \frac{1}{CL} (V_{ar} - V_0), \quad (3)$$

where A_0 is the reference cross-sectional area at the reference pressure p_0 , and C is the areal compliance. The difference $V(t) = V_{ar} - V_0$ can be calculated as

$$V(t) = V_{ar} - V_0 = \int_0^t \frac{dV_{ar}}{dt} dt = \int_0^t (Q_{in} - Q) dt, \quad (4)$$

and expression for the p becomes:

$$p = p_0 + \frac{1}{CL} \int_0^t (Q_{in} - Q) dt + \frac{\eta}{L} (Q_{in} - Q). \quad (5)$$

If we assume that constants p_0 , C , η , and L are known, and we take for Q the peripheral blood flow rate (in the first approximation it can be considered as the mean value of Q_{in}), then p is defined uniquely by the aortic valve blood flow Q_{in} . It is visible from Equation (5) that for $Q_{in} > Q$ the p is greater than p_e , and for $Q_{in} < Q$, it is smaller.

Figure 2, shows an example of calculated values of the total and elastic part of pressure. Curves in panel (a) show the input blood flow Q_{in} through aortic valve (blue line) and the blood flow Q to the peripheral vascular beds (red line), which are obtained by digitization of data from [4]. The time interval B–D represents the filling phase of the aorta ($Q_{in} > Q$) during which the cross-sectional area and volume increase. Outside this interval, aorta is emptying and cross-sectional area and volume decrease. Panel (b) shows the net blood flow rate into the chamber, and integrated time variation of the chamber volume, according to Equation (4). Panel (c) shows the calculated elastic part of pressure p_e (blue line), which is proportional with $V(t)$, and the total pressure p (green line), calculated according to Equation (5). It can be seen that $p = p_e$ at points B and D, within the time interval B–D $p > p_e$, and outside the B–D interval, when $Q_{in} < Q$, and $p < p_e$. The biggest positive difference $p - p_e$ (the biggest viscous part of pressure) is at point close to point C, when the difference between Q_{in} and Q is the biggest, and the biggest negative differences are at a point close to point F. It should be noted that the curve of elastic part of the pressure is smooth, while the total pressure curve shows an incisure, due to changes in the viscous part of the pressure. During the time interval D–E–F the difference $Q_{in} - Q$ is negative and it increases in magnitude, and consequently the total pressure becomes much smaller than the elastic part of the pressure. This pressure drop in the viscous part of pressure forms the left branch of the incisure. During the time interval F–G the negative difference $Q_{in} - Q$ becomes smaller in magnitude, and total pressure becomes closer to the elastic part of pressure, forming the right branch of the incisure. It is clear that the bigger value of η will cause the deeper incisure.

In the following sections of the paper, we will check the influence of the arterial wall viscosity on the depth of the incisure, by applying the one-dimensional mathematical model to the simplified arterial tree, which consists of 37 large arteries.

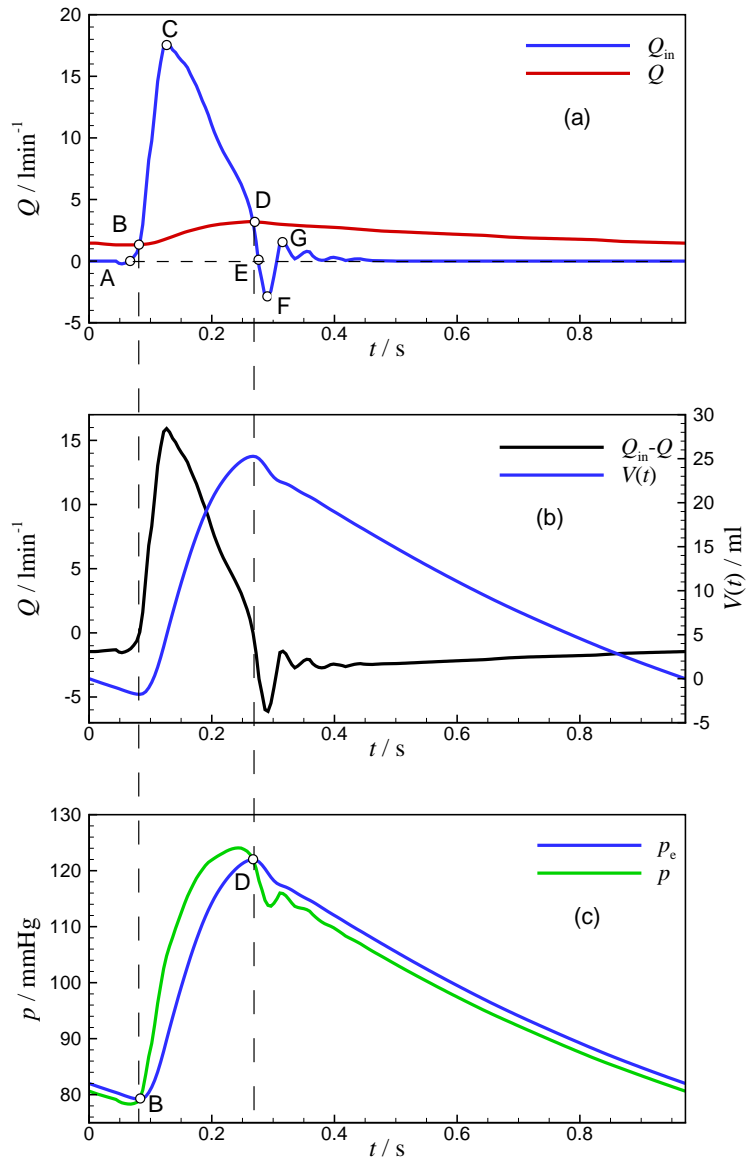


Figure 2: Filling and emptying phases of the aortic root. Curves in the diagram (a) are the result of data digitization from [4]

3 Mathematical Model of One-Dimensional Blood Flow

The arterial tree composed of large arteries is considered, which starts at the aortic root and ends at a certain level of branching arteries. In large arteries blood flow is assumed to be one-dimensional, and the peripheral vascular bed is modelled by the

resistor. The non-linear one dimensional model of arterial flow in the impermeable blood vessel is defined by:

$$\frac{\partial A}{\partial t} + \frac{\partial Q}{\partial x} = 0, \quad (6)$$

$$\frac{\partial Q}{\partial t} + \frac{A}{\rho} \frac{\partial p}{\partial x} + \frac{\partial(Qv)}{\partial x} = -fQ, \quad (7)$$

$$p = p_e(A) + \eta \frac{\partial A}{\partial t}, \quad (8)$$

where x is the space coordinate, t is the time coordinate, $A = A(x,t)$ is the circular cross-sectional area of the blood vessel, $Q = Q(x,t)$ is the volume flow rate, $p = p(x,t)$ is the transmural pressure, $v = Q/A$ is the mean blood flow velocity, ρ is the constant blood density, f is the friction coefficient, $p_e = p_e(A)$ is the elastic part of transmural pressure, and η is the viscous resistance of the wall defined by [5]:

$$\eta = \frac{2\sqrt{\pi}\varphi\delta}{3A_0\sqrt{A}}, \quad (9)$$

where φ is the wall viscosity, δ is the arterial wall thickness, and A_0 is the reference cross-sectional area at the reference pressure p_0 . The friction coefficient f is defined by formula [6]:

$$f = \frac{2(\zeta+2)\pi\mu}{\rho A}, \quad (10)$$

where μ is the fluid viscosity and ζ is the velocity profile order (here, $\zeta = 9$).

The constitutive equation, which relates the elastic part of pressure and the blood vessel diameter [7] is:

$$p_e = p_0 + \frac{1}{C_D}(\sqrt{A} - \sqrt{A_0}) \quad (11)$$

where C_D is defined by the formula:

$$C_D = \frac{3A_0}{4\sqrt{\pi}E\delta}, \quad (12)$$

where E is Young's modulus. From Equation (11) follows the relation between the areal compliance $C = dA/dp_e$ and C_D :

$$C = 2C_D\sqrt{A}. \quad (13)$$

By definition, the speed of sound is:

characteristic lines defined by $\xi^+ = dx/dt = v + c$ and $\xi^- = dx/dt = v - c$. The compatibility equations are:

$$\frac{1}{C} \frac{dQ^+}{dt} - (v - c) \frac{dp^+}{dt} = -\frac{1}{C} fQ - v^2 \eta \frac{\partial^2 A}{\partial x \partial t} + (v - c) \eta \frac{\partial^2 Q}{\partial x \partial t}, \quad (16)$$

$$\frac{1}{C} \frac{dQ^-}{dt} - (v + c) \frac{dp^-}{dt} = -\frac{1}{C} fQ - v^2 \eta \frac{\partial^2 A}{\partial x \partial t} + (v + c) \eta \frac{\partial^2 Q}{\partial x \partial t}, \quad (17)$$

where, for example, $dQ^\pm / dt = \partial Q / \partial t + (v \pm c) \partial Q / \partial x$, and dQ^+ and dQ^- are discretized in the form: $dQ^+ = Q_R^n - \bar{Q}_F$ and $dQ^- = Q_L^n - \bar{Q}_B$ (see notation in Figure 3, overbar denotes interpolated values).

The blood flow rate Q_{Wj} toward the peripheral vascular bed is defined by the resistance R_{Wj} as shown in Figure 4, by the equation

$$p_j - p_{out} = R_{Wj} Q_{Wj}, \quad (18)$$

where p_{out} is the peripheral pressure, which is defined as the transmural pressure.

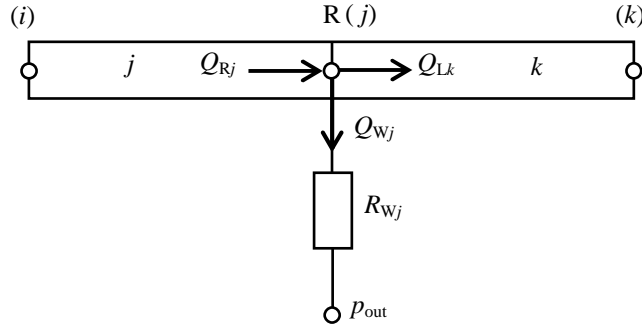


Figure 4: Model of blood flow rate Q_{Wj} toward the peripheral vascular bed

In each node the continuity equation holds, for example, for the node R in Figure 4, it is:

$$Q_{Rj} = \frac{p_j - p_{out}}{R_{Wj}} + Q_{Lk}. \quad (19)$$

After discretization of Equations (16) and (17), a set of algebraic equations is obtained. Due to non-linearity of the mathematical model, the solution procedure is an iterative one. The iteration stops when differences in pressure in two successive iterations become less than 0.0133 Pa, in all nodes of the arterial tree. In the input node (denoting the exit from the aortic valve) it is possible to prescribe the pressure or flow rate, and the initial conditions are $Q = 0$, $A = A_0$ and $p = p_0$. Since we are interested in the periodic flow regime, the integration time should be long enough to diminish the influence of initial conditions. Detailed description of the method can be found in [8].

5 Results and Discussion

In Ref. [8], the numerical method is carefully verified in a series of tests and the mathematical model is validated by using experimental results of a silicone model of the arterial tree consisting of 37 large arteries [9] as shown in Figure 5. Arterial wall is viscoelastic: with $E=1.2$ MPa, and $\varphi=3\pm 0.3$ kPa·s. All necessary data of this test are provided in the Supplementary material of [9], and Table 1 reviews some of them. Here, we use this problem to analyze the influence of the wall viscosity on the enclosure. For this purpose, we will calculate the blood flow in the 37-element arterial tree with three different retardation constants $\tau=\eta C=\varphi/E=10, 30,$ and 50 ms (it is reasonable to assume that a real arterial wall is more viscous than silicone (the retardation time constant of silicone is $\tau=2.5\pm 0.25$ ms)). For the purpose of numerical procedure, we discretized the arterial tree into 860 elements. At the ends of arterial tree the outflow boundary condition is defined by the resistor of resistance R_w , as reported in Table 1. The mathematical model was integrated for a sufficient number of heart periods to achieve beat-to-beat repeatability of the pressure profile, and the results from the last period are analyzed.

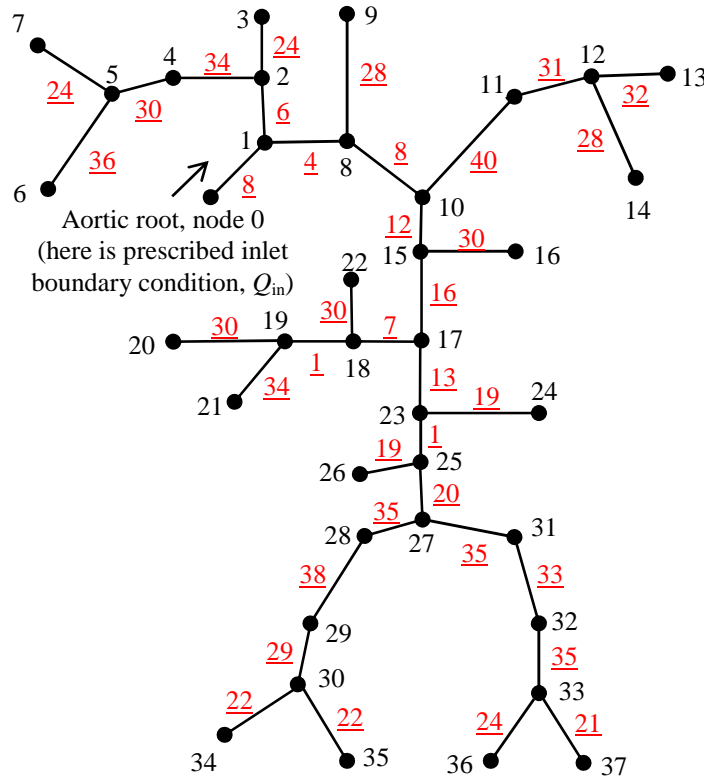


Figure 5: Scheme of the 37-artery model. Black circles denote inlet/output nodes. At the input node (node 0), we prescribe the aortic valve blood flow [9]. The segment number corresponds to the number of its output node. Underlined red numbers denote the number of segment divisions for the purpose of the numerical method

Table 1: Some parameters of 37-artery model

Property	37-artery network	
Input periodical blood flow, Q_{in} (m^3/s)	[9]	
Blood density, ρ (kg/m^3)	1050	
Blood viscosity, μ (mPa·s)	2.5	
Initial pressure, p_0 (kPa)	0	
Retardation time constant, $\tau = \eta C = \phi / E$ (ms)	10	
	30	
	50	
Outflow pressure, p_{out} (Pa)	432.6	
Velocity profile order, ζ	9	
Arterial length (m)	Min	0.007
	Max	0.245
Segment radius at the reference pressure (mm)	Min	1.55
	Max	14.4
Speed of sound at the reference pressure (m/s)	Min	4.84
	Max	14.9
Resistance R_w in the Windkessel model ($GPa \cdot s/m^3$)	3 - Right carotid	2.67
	6 - Right radial	3.92
	7 - Right ulnar	3.24
	9 - Left carotid	3.11
	13 - Left radial	3.74
	14 - Left ulnar	3.77
	16 - Intercostals	2.59
	20 - Splenic	3.54
	21 - Gastric	4.24
	22 - Hepatic	3.75
	24 - Left renal	3.46
	26 - Right renal	3.45
	34 - Right anterior tibial	5.16
35 - Right posterior tibial	5.65	
36 - Left posterior tibial	4.59	
37 - Left anterior tibial	3.16	

Figure 6 shows the aortic valve flow rate (Q_{in}), which is used as the inlet boundary condition at the inlet node and the aortic root pressure-time variation obtained by different values of the retardation time constant (i.e. different values of the arterial wall viscosity). In addition, the definition of the incisure depth is shown. It is visible that increase in the arterial wall viscosity results in an increase in the depth of the incisure, which is in accordance with the hypothesis. Also, the increase in the arterial wall viscosity results in an increase in the slope of the pressure curve at the beginning of ejection, as well as in an increase in the systolic pressure, which is well known in the clinical practice.

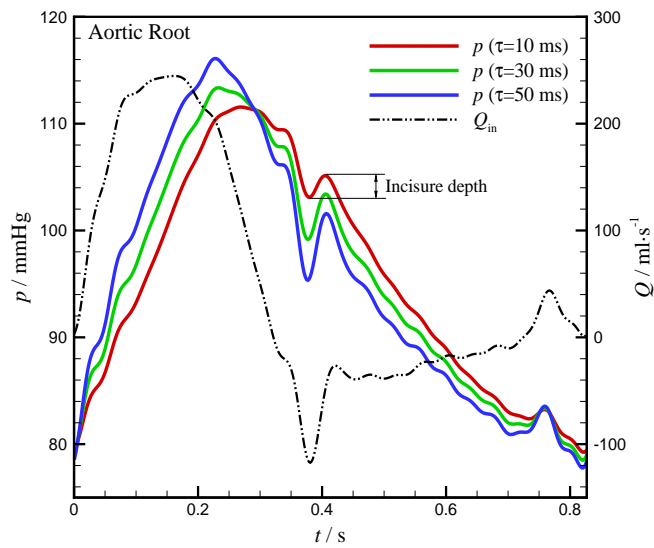


Figure 6: Aortic valve flow rate and the aortic root pressure versus time for different arterial wall viscosity

It is also known that the pressure shape changes along the aorta in a way that the systolic pressure increases, while the diastolic pressure remains constant or slightly decreases. Figure 7 shows results for pressure at different locations along the aorta, obtained at $\tau = 30$ ms. It is visible that systolic pressure increases with distance from the aortic root.

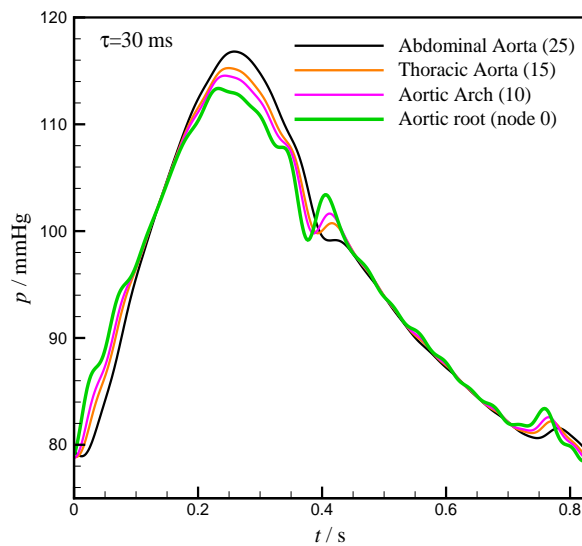


Figure 7: Results for the pressure-time variation at different location in the aorta, at $\tau = 30$ ms

It is also clear that the incisure depth decreases with the distance from the aortic root, and in the considered case of wall viscosity, the incisure disappears at the level of the abdominal aorta. Table 2 shows the incisure depth for the three values of the wall viscosity and at five locations in the arterial tree. It is visible that in the case of low arterial wall viscosity the incisure disappears in the Thoracic aorta, while in the case of higher arterial wall viscosity the incisure depth is also significant in the abdominal aorta. The fact that the incisure depth increases with the increase of the wall viscosity can have a potential value in clinical practise, providing that clinicians can estimate the aortic wall viscosity from the incisure depth. This will be of interest only in case if we can measure the incisure depth noninvasively, which is not possible for now in the aortic root. The closest place to the aortic root, where we can measure the pressure noninvasively, is the neck (the position of the Left and Right Carotid). The main question is if the incisure depth is still significant at those positions. It is visible from Table 2 that the incisure depth at those positions is somewhat reduced with respect to the depth at the aortic root, but it seems it is still significant for potential clinical application.

Table 2: Depth of the incisure (see definition in Figure 6) in mmHg, in case of the three different wall viscosity and at five different locations in the arterial tree

$\tau = \phi/E$ (ms)	Position				
	Aortic Root	Left Carotid	Right Carotid	Thoracic Aorta	Abdominal Aorta
10	2.0	1.5	2.1	0.0	0.0
30	4.2	2.7	3.2	0.9	0.1
50	6.2	4.5	5.0	2.8	1.3

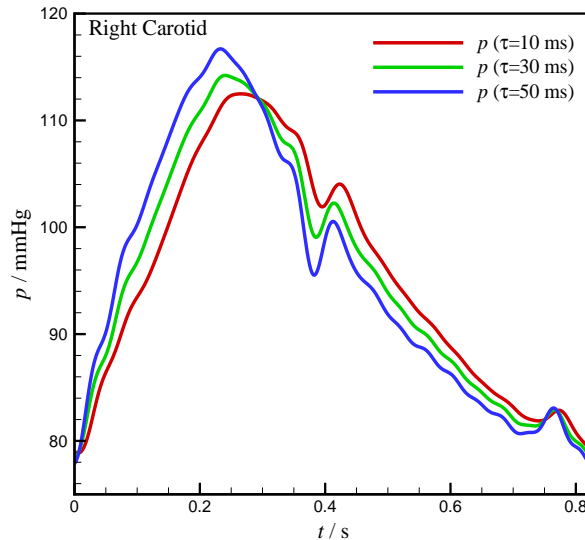


Figure 8: Right Carotid pressure versus time for different arterial wall viscosity

Figure 8 illustrates the pressure profiles at the Right Carotid in case of different values of the retardation time constant. The profiles are very similar in shape to those at the aortic root.

6 Conclusion

We simulated blood flow in a 37-artery network with a viscoelastic wall (the Voigt model), by using the one-dimensional mathematical model and numerical method of characteristics. We investigated the depth of the incisure in the pressure profile at different locations in the arterial tree with respect to the three different values of the arterial wall viscosity. Based on the obtained results we can conclude:

The increase of the arterial wall viscosity results in an increase in the incisure depth. This fact presents a certain potential for clinical estimation of the arterial wall viscosity, from the measurements of the incisure depth.

The incisure depth decreases with distance from the aortic root, but it is still significant at the positions of the Left and Right Carotid, where non-invasive pressure measurements can be performed.

References

- [1] Sabbah, H.N., Stein, P.D. Valve Origin of the Aortic Incisura. *Am J Cardiol*, **41**:32-8, 1978.
- [2] Guyton, A.C., Hall, J.E. *Textbook of Medical Physiology*. Elsevier Saunders, Philadelphia, Pennsylvania, 2006.
- [3] Nichols, W.W., O'Rourke, M.F., Vlachopoulos, C. *McDonald's Blood Flow in Arteries*. Hodder Arnold, London, UK, 2011.
- [4] Wang, J.J., O'Brien, A.B., Shrive, N.G., Parker, K.H., Tyberg, J.V. Time-domain Representation of Ventricular-arterial Coupling as a Windkessel and Wave System. *Am J Physiol Heart Circ Physiol*, **284**:1358-1368, 2003.
- [5] Alastruey, J., Khir, A.W., Matthys, K.S., et al. Pulse Wave Propagation in a Model Human Arterial Network: Assessment of 1-D Numerical Simulations Against in vitro Measurements. *J Biomech*, **40**:3476-3486, 2007.
- [6] Smith, N.P., Pullan, A.J., Hunter, P.J. An Anatomically Based Model of Transient Coronary Blood Flow in the Heart. *SIAM J. Appl. Math*, **62**:990-1018, 2002.
- [7] Formaggia, L., Lamponi, D., Quarteroni, A. One-dimensional Models for Blood Flow in Arteries. *J Eng Math*, **47**:251-276, 2003.
- [8] Korade, I. *Modeling of Blood Flow in an Arterial Tree with Viscoelastic Wall*. PhD Thesis, University of Zagreb, Faculty of Mechanical Engineering and Naval Architecture, 2017. (in Croatian)
- [9] Matthys, K.S., Alastruey, J., Peiro, J., et al. Pulse Wave Propagation in a Model Human Arterial Network: Assessment of 1-D Numerical Simulations Against in vitro Measurements. *J Biomech*, **40**:3476-3486, 2007.